

# Ferroelectric-relaxor crossover in $\text{Ba}(\text{Ti}_{1-x}\text{Zr}_x)\text{O}_3$ studied using neutron total scattering measurements and reverse Monte Carlo modeling

I.-K. Jeong,<sup>1,\*</sup> C. Y. Park,<sup>2</sup> J. S. Ahn,<sup>2</sup> S. Park,<sup>2</sup> and D. J. Kim<sup>2</sup><sup>1</sup>*Department of Physics Education & Research Center for Dielectrics and Advanced Matter Physics, Pusan National University, Busan 609-735, Korea*<sup>2</sup>*Department of Physics, Pusan National University, Busan 609-735, Korea*

(Received 26 March 2010; revised manuscript received 1 June 2010; published 22 June 2010)

Comprehensive structural studies on normal ferroelectric to relaxor crossover in  $\text{Ba}(\text{Ti}_{1-x}\text{Zr}_x)\text{O}_3$  (BTZ) are performed using neutron total scattering measurements analyzed by reverse Monte Carlo modeling. In BTZ solid solution, we estimated the degree of the displacement correlation between Ti ions and found that it is stronger and extends much longer for ferroelectric state than relaxor state. In addition, we present evidence that the overall off-centering behavior of Ti ion changes from directional to random displacements between ferroelectric and relaxor phases, and thus provide atomistic picture for ferroelectric-relaxor crossover with increasing Zr concentration.

DOI: [10.1103/PhysRevB.81.214119](https://doi.org/10.1103/PhysRevB.81.214119)

PACS number(s): 77.80.-e, 61.05.F-, 77.22.-d, 77.84.Ek

## I. INTRODUCTION

Relaxor ferroelectrics such as  $\text{Pb}(\text{Mg}_{1/3}\text{Nb}_{2/3})\text{O}_3$ - $\text{PbTiO}_3$  compounds are fascinating materials with high, relatively temperature-insensitive permittivity. In addition, lead-containing relaxors exhibit ultrahigh electromechanical coupling, and thus have been widely used in modern technological applications.<sup>1,2</sup> However, due to environmental issues, recently intense research works are being conducted in search of new lead-free relaxor materials.<sup>3-5</sup>

One of the important routes for inducing relaxor state is a chemical substitution to normal ferroelectrics. For example,  $\text{BaTiO}_3$  exhibits typical ferroelectric features with sharp dielectric response near Curie temperature. By the Zr substitution on Ti, however,  $\text{Ba}(\text{Ti}_{1-x}\text{Zr}_x)\text{O}_3$  (BTZ) solid solution undergoes normal ferroelectric (nFE) to relaxor (R) crossover around  $x \approx 0.28$  (Ref. 6) with enhanced tunability of dielectric response.<sup>7</sup> In terms of crystal structure, Zr substitution for Ti ions distorts the lattice due to the large size mismatch between  $\text{Zr}^{4+}$  (0.79 Å) and  $\text{Ti}^{4+}$  (0.68 Å). The resultant structural disorder has a drastic impact on long-range crystal symmetry of  $\text{BaTiO}_3$  as all three ferroelectric phases merge together with increasing Zr concentration and only low temperature rhombohedral phase survives at around  $x \approx 0.15$ .<sup>8</sup> This result suggests that the substitution of Zr interferes with off-centering and ordering behaviors of Ti ions<sup>9-11</sup> and dynamics of polar nanoregions.<sup>12-14</sup> Thus, for microscopic understanding of nFE-R crossover, it is crucial to clarify the role of Zr substitution on Ti off-centering behavior in BTZ solid solution.

To comprehend structural disorders caused by Zr substitution in BTZ solid solution, Zr-K edge x-ray absorption fine structure (XAFS) experiments were performed at room temperature by Laulhe *et al.*<sup>15</sup> The authors found that local structure is distinct from the average cubic structure and the atomic distance between Zr ions is independent of Zr concentration. Similar results were reported from neutron pair distribution function (PDF) analysis at room temperature.<sup>16</sup> In the PDF studies, it was found that local polarization is mainly due to the displacements of Ti ions.

Besides, the authors reported that Ti displacements are very similar between relaxor and the ferroelectric states, leaving the atomistic nature of the nFE-R crossover not well understood. In this paper, we present atomistic picture for nFE-R crossover in  $\text{Ba}(\text{Ti}_{1-x}\text{Zr}_x)\text{O}_3$  using neutron total scattering measurements<sup>17,18</sup> and reverse Monte Carlo (RMC) modeling.

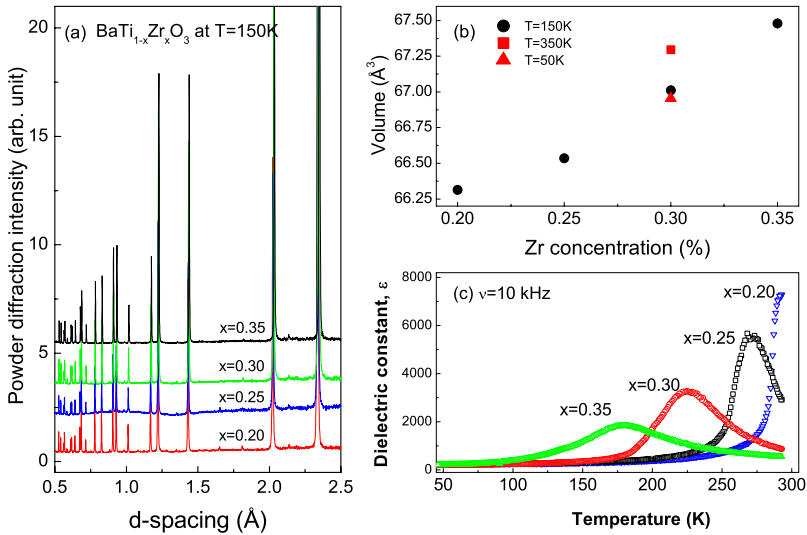
## II. EXPERIMENTS AND ANALYSIS

Powder samples of  $\text{Ba}(\text{Ti}_{1-x}\text{Zr}_x)\text{O}_3$  ( $x=0.20, 0.25, 0.30, 0.35$ ) were synthesized using the conventional solid state reaction.<sup>19</sup> Neutron powder diffraction experiments were performed on the NPDF instrument at the Los Alamos Neutron Science Center. All measurements were performed at temperature 150 K which is below the maximum temperature,  $T_m$  of the dielectric response. For  $x=0.30$  additional data were taken at 50 K and 350 K.

Experimental total scattering structure function,  $S(Q)$  which contains both Bragg and diffuse scattering was obtained up to wave vector  $Q=30 \text{ \AA}^{-1}$  from neutron powder diffraction measurements after corrections for experimental effects and normalization by incident neutron flux using program PDFgetN.<sup>20</sup> Real-space pair distribution function (PDF),  $G(r)$  is determined from a sine Fourier transform of  $S(Q)$  i.e.,  $G(r)=4\pi r[\rho(r)-\rho_0]=\frac{2}{\pi}\int_0^{Q_{\max}} Q[S(Q)-1]\sin QrdQ$ . Here,  $Q$  is a scattering wave vector,  $\rho(r)$ , and  $\rho_0$  are atomic number density and average number density, respectively. To extract information on long-range and short-range ordering both Bragg scattering and diffuse scattering are fitted simultaneously using RMC approach.<sup>21,25</sup> As Bragg scattering is originated from long-range ordering and diffuse scattering is due to a deviation from three-dimensional periodicity, the final model structure contains features of long-range and short-range ordering.

## III. RESULTS AND DISCUSSION

We first examine long-range crystal structure of  $\text{Ba}(\text{Ti}_{1-x}\text{Zr}_x)\text{O}_3$  ( $x=0.20, 0.25, 0.30, 0.35$ ) at 150 K as shown



in Fig. 1(a). No noticeable feature was observed in diffraction pattern with increasing Zr concentration except overall shift of Bragg peak positions toward higher  $d$  spacing. To obtain detailed structural information, Rietveld refinements were performed for all concentrations (not shown) using GSAS.<sup>22</sup> Figure 1(b) shows the volume of the unit cell as a function of Zr concentration. Here, we note that the volume expansion between  $x=0.25$  and  $x=0.30$  at 150 K is larger than that due to temperature change over 300 K for  $x=0.30$ . This large compositional volume expansion is due to the large size mismatch between  $Zr^{4+}$  and  $Ti^{4+}$  ions and causes significant impact on the Ti off-centering behaviors which in turn strongly influence dielectric response as shown in Fig. 1(c).

For thorough understanding on structural evolution caused by Zr substitution, we investigated the source of disorder in BTZ solid solution using total scattering analysis. Figure 2(a) shows a total scattering structure function of  $Ba(Ti_{0.8}Zr_{0.2})O_3$  at 150 K with  $Q_{max}=30 \text{ \AA}^{-1}$ . The corresponding PDF spectrum is shown in Fig. 2(b). Consistent with earlier PDF measurements,<sup>16</sup> we observe a partial overlap between negative<sup>23</sup> Ti-O and positive Zr-O bonds around  $r \sim 2 \text{ \AA}$  which indicates that average Ti-O bond length is shorter than that of Zr-O bond. In Fig. 2(b), we also compare PDF spectrum between  $x=0.20$  and  $x=0.35$ . From a Gaussian fitting for the peak at around  $r=2.87 \text{ \AA}$ , we found that PDF peak width increases from 0.207(3) to 0.217(4)  $\text{\AA}$  between  $x=0.20$  and  $x=0.35$ . Similarly, for the peak at around  $r=4.96 \text{ \AA}$  peak width increased from 0.227(3) to 0.236(2)  $\text{\AA}$ . This broadening of PDF peaks for higher Zr concentration indicates increasing structural disorder. In addition, the relative shift of peak position is getting larger as the pair distance increases. This is in contrast to  $Pb(Zn_{1/3}Nb_{2/3})O_3-xPbTiO_3$  system where local structures of  $x=0.05$  (R) and  $x=0.12$  (T) are nearly identical up to atomic pair distance  $r \sim 15 \text{ \AA}$ .<sup>24</sup> These findings suggest that short-range ordering as well as long-range crystal structure is a crucial ingredient for a proper understanding of nFE-R cross-over in BTZ solid solution.

To simultaneously fit both long- and short-range orderings we used reverse Monte Carlo (RMC) approach. The starting

model structure was  $16 \times 16 \times 16$  unit cells with orthogonal axes containing 20480 atoms. As crystal structure of  $Ba(Ti_{1-x}Zr_x)O_3$  consists of oxygen octahedra we ensured that octahedra are not distorted too much from regular shape using polyhedral constraint.<sup>25</sup> Figure 3 shows results of RMC run on  $Ba(Ti_{0.8}Zr_{0.2})O_3$  at 150 K using program RMCProfile.<sup>26</sup> Bragg scattering, PDF spectrum, and structure function  $S(Q)_{cv}$  which is convoluted by the size of model structure are simultaneously fitted. High quality of fitting on Bragg scattering ensures that the model structure is consistent with the material's long-range ordering. Besides, fittings on PDF spectrum and  $S(Q)_{cv}$  over whole range guarantee that the model structure has proper disorder due to thermal and off-centering displacements. Thus, the final model structure includes both long- and short-range features in the material.

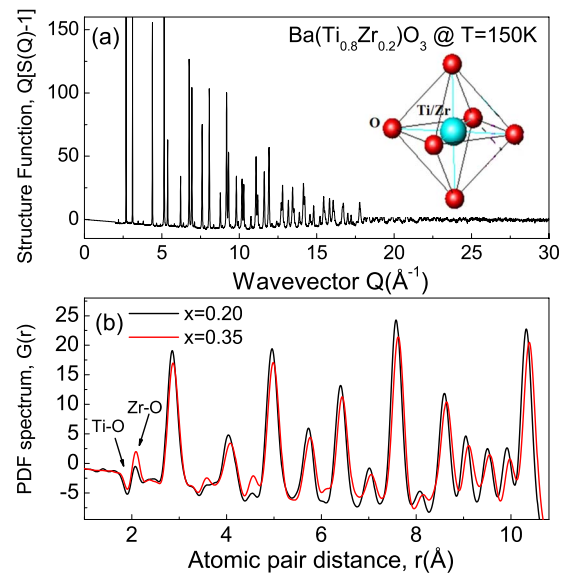


FIG. 2. (Color online) (a) Total scattering structure function,  $S(Q)$  for  $Ba(Ti_{0.8}Zr_{0.2})O_3$  at 150 K. The inset shows  $(Ti/Zr)O_6$  octahedron. (b) Comparison of PDF spectrum for  $x=0.20$  (ferroelectric) and  $x=0.35$  (relaxor) at 150 K. PDF peak positions shift toward higher- $r$  and peaks get broader for higher Zr concentration.

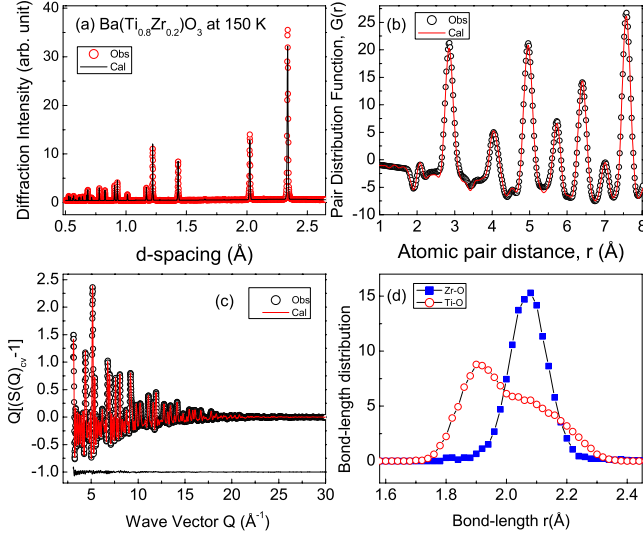


FIG. 3. (Color online) Simultaneous fitting of long- and short-range orderings in Ba(Ti<sub>0.8</sub>Zr<sub>0.2</sub>)O<sub>3</sub> at 150 K using RMC refinement. (a)–(c) show RMC fitting on Bragg peaks, PDF spectrum, and structure function, respectively.  $S(Q)_{cv}$  indicates that  $S(Q)$  is convoluted by the size of the model structure. (d) Ti-O and Zr-O bond length distributions obtained from RMC modeling.

From RMC modeling, we obtained Ti-O and Zr-O bond length distributions as shown in Fig. 3(d). Here, we found a two-peak structure for Ti-O bond in contrast to a single peak for Zr-O bond. This result confirms that Ti ions are off-centered but Zr ions stay more or less at the center of oxygen octahedra. In addition, we note that the center of bond length distribution is about 4% smaller for Ti-O bond than for Zr-O bond. Thus, we can conclude that Ti off-centering is the source of local polarization in Ba(Ti<sub>0.8</sub>Zr<sub>0.2</sub>)O<sub>3</sub> and the random distribution of TiO<sub>6</sub>/ZrO<sub>6</sub> octahedra induce lattice distortion due to their size mismatch.

Now we discuss the correlation between Ti off-center displacements in Ba(Ti<sub>0.80</sub>Zr<sub>0.20</sub>)O<sub>3</sub> and Ba(Ti<sub>0.65</sub>Zr<sub>0.35</sub>)O<sub>3</sub> which exhibit normal ferroelectric and relaxor behaviors, respectively. The degree of the displacement correlation is calculated using the correlation coefficient  $c_{ij}$  which is defined as  $c_{ij} = \langle x_i x_j \rangle / \sqrt{\langle x_i^2 \rangle \langle x_j^2 \rangle}$ .<sup>27</sup> Here  $x_i$  is the displacement of the atom on site  $i$  from the average position and  $\langle \rangle$  represents the average over the crystal. Positive, negative, and zero  $c_{ij}$  imply that ions displace in the same direction, opposite direction, and random direction, respectively.<sup>28</sup> Table I shows the displacement correlation  $c_{ij}$  between Ti ions in crystal structure of Ba(Ti<sub>0.80</sub>Zr<sub>0.20</sub>)O<sub>3</sub> and Ba(Ti<sub>0.65</sub>Zr<sub>0.35</sub>)O<sub>3</sub> calculated using program DISCUS.<sup>29</sup> Here, we note that the correlation is stronger and extends much longer for ferroelectric state than relaxor. Nevertheless, the correlation quickly decays beyond 2–3 unit cell distances for both cases. Based on these results, we speculate that BTZ solid solution is composed of polar nanoregions<sup>30–32</sup> whose polarization direction evolves on every few nanometer length scale.

To estimate the overall off-centering behavior of Ti ions, we calculated the probability of finding Ti ion on [100]-[010] plane for Ba(Ti<sub>0.80</sub>Zr<sub>0.20</sub>)O<sub>3</sub> as shown in Fig. 4(a). For this, all Ti ions in  $16 \times 16 \times 16$  unit cells are displaced into one

TABLE I. Displacement correlation coefficient  $c_{ij}$  between Ti ions in Ba(Ti<sub>0.80</sub>Zr<sub>0.20</sub>)O<sub>3</sub> and Ba(Ti<sub>0.65</sub>Zr<sub>0.35</sub>)O<sub>3</sub> at  $T=150$  K.  $c_{ij}$  is defined as  $c_{ij} = \langle x_i x_j \rangle / \sqrt{\langle x_i^2 \rangle \langle x_j^2 \rangle}$ . Here  $x_i$  is the displacement of the atom on site  $i$  from the average position and  $\langle \rangle$  represents the average over the crystal. In the table,  $n$  is an integer multiplied to vectors.

$n$	direction	Ba(Ti <sub>0.80</sub> Zr <sub>0.20</sub> )O <sub>3</sub>	Ba(Ti <sub>0.65</sub> Zr <sub>0.35</sub> )O <sub>3</sub>
		Correlation coefficient $c_{ij}$	
1	$\langle 100 \rangle$	0.424(1)	0.297(2)
	$\langle 110 \rangle$	0.314(1)	0.245(2)
	$\langle 111 \rangle$	0.217(3)	0.120(1)
2	$\langle 100 \rangle$	0.254(2)	0.128(2)
	$\langle 110 \rangle$	0.137(2)	0.031(2)
	$\langle 111 \rangle$	0.062(1)	0.012(2)
3	$\langle 100 \rangle$	0.271(2)	0.144(4)
	$\langle 111 \rangle$	0.085(1)	0.035(3)
	$\langle 111 \rangle$	0.001(2)	0.010(1)

unit cell and total number of ions is normalized to one. In addition, approximately 350 equivalent atomic configurations from RMC runs are averaged to improve statistics. As atomic coordinates from RMC modeling contain components of both thermal disorders as well as off-centering displacements, the average Ti distribution reflects both contributions. Typically, thermal disorder can be modeled using an ellipsoidal distribution.<sup>33</sup> Thus, if off-centering contribution has a distinctive feature, then it will not interfere with the thermal contribution. In Fig. 4(a), we notice that the probability is much higher on a certain position than all other places. This feature is shown better in the corresponding contour plot where the highest value is observed on the lower left side. From the result, we can conclude that local Ti off-center displacements are toward more or less diagonal direction with magnitude about 0.2 Å.

In comparison, we found that Ti off-centering behavior in relaxor Ba(Ti<sub>0.65</sub>Zr<sub>0.35</sub>)O<sub>3</sub> is rather different. As shown in Fig. 4(b) the probability is lower at the central part than that of the surrounding ridge and the height of the ridge is almost same at all directions. The corresponding contour plot shows a clearer picture. Here, it is obvious that the central part has a lower contour value than the neighboring part which is more or less circular with almost same contour value. This result indicates that local Ti off-centering is random and disordered in the relaxor state. We expect that the random displacement of Ti ions is closely related to the lattice expansion due to Zr substitution. Lattice expansion caused by a mixed distribution of larger ZrO<sub>6</sub> and smaller TiO<sub>6</sub> locally distorts oxygen octahedra due to the oxygen corner sharing. As a result, local symmetry of Ti ions are different from unit cell to unit cell and off-centered Ti ions have overall random distribution. The crossover from directional to random displacement is continuous as suggested by the gradual broadening of temperature dependent dielectric response with increasing Zr concentration.<sup>6</sup>

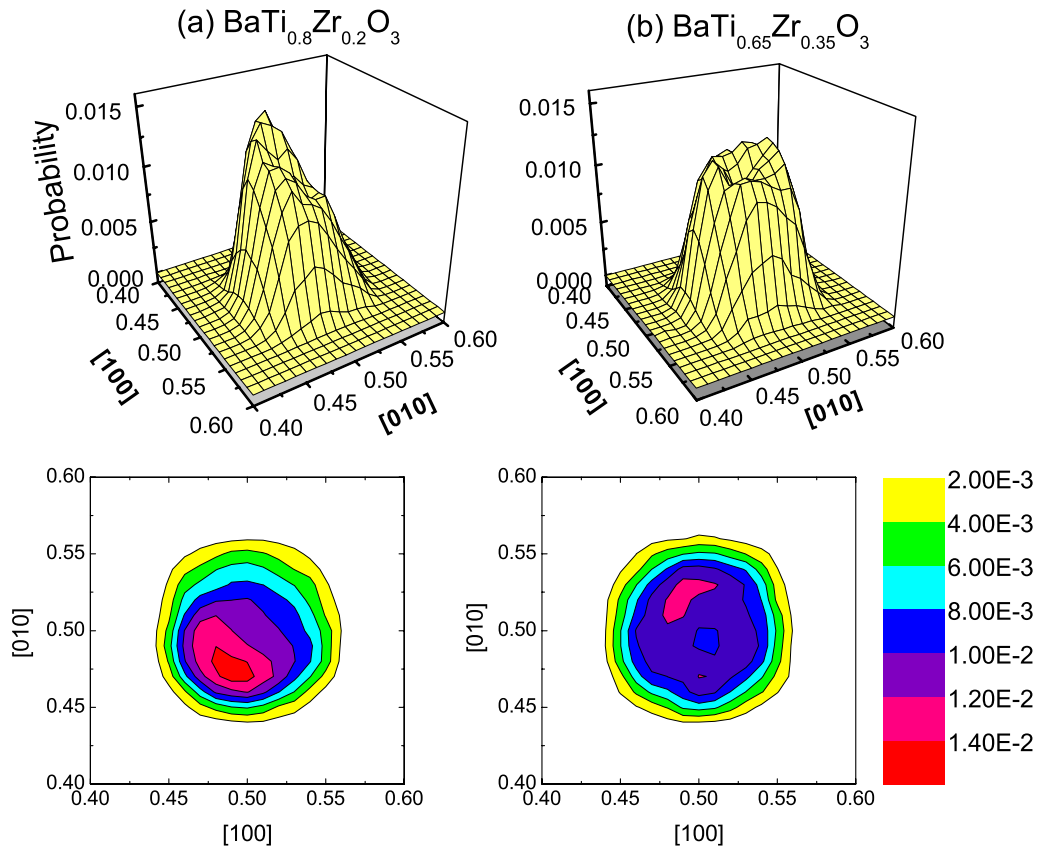


FIG. 4. (Color online) Probability of finding Ti ion on [100]-[010] plane at  $T=150$  K obtained from RMC modeling of (a)  $\text{Ba}(\text{Ti}_{0.8}\text{Zr}_{0.2})\text{O}_3$  and (b)  $\text{Ba}(\text{Ti}_{0.65}\text{Zr}_{0.35})\text{O}_3$ . Ti off-centering is directional in ferroelectric state in contrast to random displacements in relaxor state. Corresponding contour plots are also shown.

#### IV. CONCLUSION

The overall change in the off-centering behavior of Ti ion from directional to random displacements provides atomistic picture for the crossover from ferroelectric to relaxor states in BTZ solid solution with increasing Zr concentration. At low Zr concentration, the ordered off-centering of Ti ions is similar to that observed in low temperature rhombohedral  $\text{BaTiO}_3$  (Ref. 34) explaining the ferroelectric nature. On the other hand, the disordered off-centering at high Zr concentration results in the relaxor state<sup>35</sup> due to the frustrated interaction between local polarizations. Besides, the order-disorder picture provides good explanation for a distinct response in specific heat between  $\text{Ba}(\text{Ti}_{0.65}\text{Zr}_{0.35})\text{O}_3$  and prototypical relaxor materials like  $\text{Pb}(\text{Mg}_{1/3}\text{Nb}_{2/3})\text{O}_3$ . In  $\text{Pb}(\text{Mg}_{1/3}\text{Nb}_{2/3})\text{O}_3$ , a broad anomaly in specific heat appears due to an order-disorder type ordering of local polarizations.<sup>36</sup> In contrast, no such anomaly was observed in

$\text{Ba}(\text{Ti}_{0.65}\text{Zr}_{0.35})\text{O}_3$  relaxor<sup>37</sup> as much weaker ordering of local polarization develops as we presented in Fig. 4(b).

#### ACKNOWLEDGMENTS

We gratefully acknowledge discussions on RMC modeling with Matt Tucker. This work was supported by the Korea Research Foundation Grant funded by the Korean Government (Grants No. KOSEF-R01-2008-000-21092-0 and No. KRF-2006-005-J02804). Neutron diffraction measurements have benefited from the use of NPDF at the Lujan Center at Los Alamos Neutron Science Center, funded by DOE Office of Basic Energy Sciences. Los Alamos National Laboratory is operated by Los Alamos National Security LLC under DOE Contract No. DE-AC52-06NA25396. The upgrade of NPDF has been funded by NSF through Grant No. DMR 00-76488.

\*To whom correspondence should be addressed; jeong@pusan.ac.kr

<sup>1</sup>G. A. Samara, *J. Phys.: Condens. Matter* **15**, R367 (2003).

<sup>2</sup>R. E. Cohen, *Nature (London)* **441**, 941 (2006).

<sup>3</sup>R. Ravez and A. Simon, *Eur. Phys. J.: Appl. Phys.* **11**, 9 (2000).

<sup>4</sup>R. Mani, S. N. Achary, K. R. Chakraborty, S. K. Deshpande, J. E. Joy, A. Nag, J. Gopalakrishnan, and A. K. Tyagi, *Adv. Mater.* **20**, 1348 (2008).

<sup>5</sup>J. Rodel, W. Jo, K. T. P. Seifert, E. Anton, and T. Granzow, *J. Am. Ceram. Soc.* **92**, 1153 (2009).

- <sup>6</sup>A. Simon, J. Ravez, and M. Maglione, *J. Phys.: Condens. Matter* **16**, 963 (2004).
- <sup>7</sup>T. Maiti, R. Guo, and A. S. Bhalla, *Appl. Phys. Lett.* **90**, 182901 (2007).
- <sup>8</sup>Z. Yu, R. Guo, and A. S. Bhalla, *J. Appl. Phys.* **88**, 410 (2000).
- <sup>9</sup>W. Cochran, *Adv. Phys.* **9**, 387 (1960).
- <sup>10</sup>B. Zalar, V. V. Laguta, and R. Blinc, *Phys. Rev. Lett.* **90**, 037601 (2003).
- <sup>11</sup>E. A. Stern, *Phys. Rev. Lett.* **93**, 037601 (2004).
- <sup>12</sup>P. M. Gehring, S. Wakimoto, Z.-G. Ye, and G. Shirane, *Phys. Rev. Lett.* **87**, 277601 (2001).
- <sup>13</sup>J. Toulouse, D. La-Orautapong, and O. Svitelskiy, *Ferroelectrics* **302**, 271 (2004).
- <sup>14</sup>W. Dmowski, S. B. Vakhrushev, I.-K. Jeong, M. P. Hehlen, F. Trouw, and T. Egami, *Phys. Rev. Lett.* **100**, 137602 (2008).
- <sup>15</sup>C. Laulhe, F. Hippert, J. Kreisel, M. Maglione, A. Simon, J. L. Hazemann, and V. Nassif, *Phys. Rev. B* **74**, 014106 (2006).
- <sup>16</sup>C. Laulhe, F. Hippert, R. Bellissent, A. Simon, and G. J. Cuello, *Phys. Rev. B* **79**, 064104 (2009).
- <sup>17</sup>T. Egami and S. J. L. Billinge, *Underneath the Bragg Peaks: Structural Analysis of Complex Materials* (Pergamon Press, Oxford, UK, 2003).
- <sup>18</sup>I.-K. Jeong, T. W. Darling, J. K. Lee, T. Proffen, R. H. Heffner, J. S. Park, K. S. Hong, W. Dmowski, and T. Egami, *Phys. Rev. Lett.* **94**, 147602 (2005).
- <sup>19</sup>J. Ravez and A. Simon, *Eur. J. Solid State Inorg. Chem.* **34**, 1199 (1997).
- <sup>20</sup>P. F. Peterson, M. Gutmann, T. Proffen, and S. J. L. Billinge, *J. Appl. Crystallogr.* **33**, 1192 (2000).
- <sup>21</sup>R. L. McGreevy, *J. Phys.: Condens. Matter* **13**, R877 (2001).
- <sup>22</sup>A. C. Larson and R. B. Von Dreele, Los Alamos National Laboratory, Report No. LAUR 86-748, 1986 (unpublished).
- <sup>23</sup>G. L. Squires, *Introduction to the Theory of Thermal Neutron Scattering* (Dover Publications Inc., New York, 1996).
- <sup>24</sup>I.-K. Jeong, *Phys. Rev. B* **79**, 052101 (2009).
- <sup>25</sup>M. G. Tucker, M. T. Dove, and D. A. Keen, *J. Appl. Crystallogr.* **34**, 630 (2001).
- <sup>26</sup>M. G. Tucker, D. A. Keen, M. T. Dove, A. L. Goodwin, and Q. Hui, *J. Phys.: Condens. Matter* **19**, 335218 (2007).
- <sup>27</sup>R. B. Neder and T. Proffen, *Diffuse Scattering and Defect Structure Simulations—A Cook Book Using the Program DISCUS* (Oxford University Press, Oxford, 2007).
- <sup>28</sup>I.-K. Jeong, Th. Proffen, F. Mohiuddin-Jacobs, and S. J. L. Billinge, *J. Phys. Chem. A* **103**, 921 (1999).
- <sup>29</sup>Th. Proffen and R. Neder, *J. Appl. Crystallogr.* **30**, 171 (1997).
- <sup>30</sup>H. You and Q. M. Zhang, *Phys. Rev. Lett.* **79**, 3950 (1997).
- <sup>31</sup>T. R. Welberry, M. J. Gutmann, H. Woo, D. J. Goossens, G. Xu, C. Stock, W. Chen, and Z.-G. Ye, *J. Appl. Crystallogr.* **38**, 639 (2005).
- <sup>32</sup>G. Xu, Z. Zhong, Y. Bing, Z.-G. Ye, and G. Shirane, *Nature Mater.* **5**, 134 (2006).
- <sup>33</sup>W. Massa, *Crystal Structure Determination* (Springer, Berlin, 2000).
- <sup>34</sup>Q. Zhang, T. Cagin, and W. A. Goddard III, *Proc. Natl. Acad. Sci. U.S.A.* **103**, 14695 (2006).
- <sup>35</sup>B. E. Vugmeister and M. D. Glinchuk, *Rev. Mod. Phys.* **62**, 993 (1990).
- <sup>36</sup>Y. Moriya, H. Kawaji, T. Tojo, and T. Atake, *Phys. Rev. Lett.* **90**, 205901 (2003).
- <sup>37</sup>M. Nagasawa, H. Kawaji, T. Tojo, and T. Atake, *Phys. Rev. B* **74**, 132101 (2006).